

## Mathematical modeling of transient processes in a section of open-phase power grid

**Abstract.** Relying on the fundamental laws of applied electric engineering, a mathematical model is developed of a power grid section that consists of a supply line and a three-phase power transformer. The line is represented as a resistance-induction-volume element supplied from an asymmetrical electromotive force (EMF) system source, the transformer as non-linear electromagnetic circuits. This model serves the purpose of analysing the object's transient states, including its open-phase state.

**Streszczenie.** W pracy niniejszej wychodząc z podstawach praw elektrotechniki stosowanej opracowano model matematyczny fragmentu sieci elektroenergetycznej, który składa się z linii zasilania oraz trójfazowego transformatora mocy. Linia przedstawiona jest, jako rezystancyjno-indukcyjno-pojemnościowy element, zasilany przez źródło asymetrycznego układu sił elektromotorycznych SEM. Transformator mocy przedstawiony jest, jako nieliniowy element w postaci elektromagnetycznych obwodów. Za pomocą tego modelu analizowane są stany przejściowe układu, w tym stan niepełnofazowy. (Modelowanie matematyczne procesów niestabilnych w fragmencie sieci energetycznej w stanach niepełnofazowych).

**Keywords:** mathematical modelling, power grid, transformer, transient processes, transmission line equations, open-phase state.

**Słowa kluczowe:** modelowanie matematyczne, sieć energetyczna, transformator, procesy przejściowe, równania linii przesyłowych, stan niepełnofazowy.

### Introduction

Power grids are among the crucial strategic facilities of any state. Their very important role consists in transmitting electromagnetic energy over long distances. Depending on voltage classes, these distances can range widely, from several to several hundred kilometres.

Historically, energy has been transmitted over three-phase networks. This means, in the normal state, electricity is transmitted by means of a symmetrical system of three-phase voltages. In the process of power supply, however, a variety of interferences are possible, both from a supply line and electric equipment included in a power system.

The supply line's open-phase operation is a common interference, beside a variety of short-circuiting types. From the perspective of applied power engineering, these are usually treated as emergency conditions that trigger automatic safety devices. In Figure 1, the line is supplied with an earthed neutral two-phase power. The system is never short-circuited and electricity receivers are only supplied with two phases. The question arises, how long can such a situation be continued? This depends on the receivers' power and the power reserves of the primary energy source.

This is possible if Y/ $\Delta$  winding group transformers are used. Such connections are known to provide best system symmetrisation in asymmetric grid operation.

Experimenting with main transmission lines is obviously very difficult and highly costly. Therefore, we suggest using the mathematical modelling apparatus to analyse the subject matter as it allows investigations without a need for costly experimentation in real conditions. We have already developed some adequate mathematical models of power grids [1, 2]. In this paper, meanwhile, we analyse a mathematical model of a power transformer introduced to a high-voltage grid.

The analysis of transient processes in power grids is highly topical, as evidenced by the numbers of scientific publications worldwide. Let's review some that are most applicable to this paper from the perspective of transformer modelling.

Research in this field should be divided into two types.

The first involves software complexes including ready-made mathematical models of electric grid elements or utilises these software components to produce such models. [3], describing a mathematical model of a single-phase superconducting transformer implemented to *Pspice*, belongs here. *EMTP/ATP* software complex serves to analyse transient processes in electric grid elements in [4] and [5]. The model presented in [6] bases on differential equation theory and is implemented as structural diagrams to *Matlab/Simulink* software complex.

The other type of publications concerns the applications of circuit and field (field-circuit) models of grid elements in line with the theory of ordinary and partial differential equations. The authors of [7] have accordingly developed a mathematical model of a  $\Delta/Y$  winding group transformer. The model is described with a system of non-linear differential equations. A model of triple-winding transformer is similarly described in [8]. Based on a mathematical transformer model, calculations for and peculiarities of asymmetrical operation states are presented in [9] of a transformer including a circuit with three magnetic rods. In [10], a grid's mathematical model is prepared to analyse flux distributions with a view to optimum electricity consumption.

Thus, multiple publications have addressed the development of mathematical transformer models, whereas scant attention has been paid to the open-phase operation states of power transformers as power grid elements.

**The aim of this paper** is to model transient electromagnetic processes in a grid section which consists of an electric line supplied with symmetrical three-phase voltages and a power transformer connected to an asymmetric load.

### A mathematical model of a power grid section

The supply line model is an electric circuit with R-L-C in series-parallel connections and a symmetrical system of supply voltages as EMFs, as shown in Figure 1.

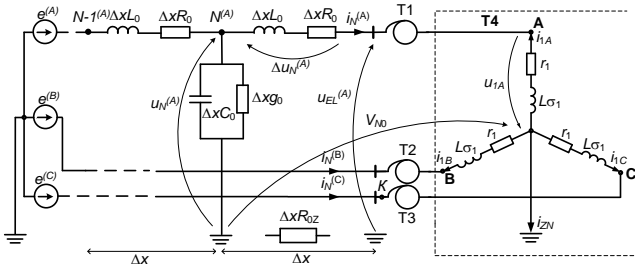


Fig. 1. A calculation diagram of power supply line and primary power transformer winding

The power transformer's model is presented as electromagnetic circuits of non-linear magnetising curves. The star-triangle ( $Y/\Delta$ ) arrangement serves as an example of winding connection. The primary windings are connected into a Y and the secondary windings into a triangle  $\Delta$  and connected to a series-parallel R-L-C load. Three single autotransformers, T1 – T3, are placed between the power line and a three-phase transformer T4, cf. Fig. 1, and their parameters are addressed in T4's computer simulations by connecting them in series and reflecting T4's ratio.

A calculation diagram of the primary power transformer winding and equivalent load are illustrated in Figure 2.

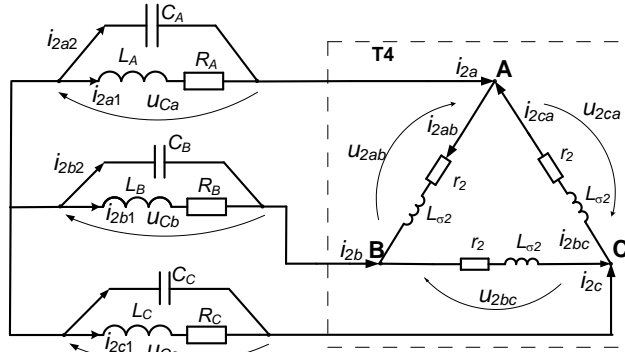


Fig. 2. A calculation diagram of the primary power transformer winding and equivalent load

Based on Kirchhoff's second law, the equations for the primary and secondary transformer windings and for stationary connections will be written:

$$(1) \frac{d\Psi_{1j}}{dt} = u_{T1j} - r_1 i_{1j}, \quad \Psi_A + \Psi_B + \Psi_C = \Psi_0;$$

$$(2) \Psi_{1A} + \Psi_{1B} + \Psi_{1C} = \Psi_{10}, \quad i_{1A} + i_{1B} + i_{1C} \neq 0;$$

where:  $u_{1j}, u_{1Cj}$  – the phase voltages of the primary transformer winding and electric power line,  $\Psi_{1j}$  – the full coupled fluxes of the primary winding phases,  $r_1$  – phase resistance,  $i_{1j}$  – phases current.

If coupled fluxes across a power transformer aren't compensated, the transformer model is substantially more complicated. For this reason, we use one of the most successful models, published in [11]:

$$(3) \frac{d\mathbf{i}_1}{dt} = \mathbf{A}_{11}(\mathbf{u}_1 - \mathbf{r}_1 \mathbf{i}_1) + \mathbf{A}_{12}(\mathbf{u}_2 - \mathbf{r}_2 \mathbf{i}_2);$$

$$(4) \frac{d\mathbf{i}_2}{dt} = \mathbf{A}_{21}(\mathbf{u}_1 - \mathbf{r}_1 \mathbf{i}_1) + \mathbf{A}_{22}(\mathbf{u}_2 - \mathbf{r}_2 \mathbf{i}_2);$$

where:  $\mathbf{A}_{ij}$  – matrixes dependent on reverse dissipation inductances and the magnetization of power transformer.

The expanded state equations of the transformer will be expressed in the matrix-vectorial form addressing the supply line's effects, see Figures 1 and 2 and monograph [11].

$$(5) \frac{d\mathbf{i}_N}{dt} = (\mathbf{1} + \Delta x \mathbf{L}_0)^{-1} \left[ \mathbf{A}_{11}(\mathbf{u}_N - (\Delta x \mathbf{R}_0 + \mathbf{r}_1) \mathbf{i}_N + \mathbf{V}_0) + \mathbf{A}_{12}(\mathbf{B}_1 \mathbf{B}_2 \mathbf{u}_2 - \mathbf{r}_2 \mathbf{B}_1 \mathbf{i}_{2L}) \right];$$

$$(6) \frac{d\mathbf{i}_{2L}}{dt} = \mathbf{D}_1 \mathbf{u}_N + \mathbf{D}_2 \mathbf{u}_2 + \mathbf{D}_3 \mathbf{V}_0 + \mathbf{D}_4 \mathbf{i}_N + \mathbf{D}_5 \mathbf{i}_{2L},$$

where:  $\mathbf{D}$  system parameter matrices,  $\mathbf{B}_1, \mathbf{B}_2$  – topological matrices.

Voltage across the power transformer load is calculated in the usual manner, see Fig. 2:

$$(7) \frac{d\mathbf{u}_2}{dt} = \mathbf{C}_2^{-1}(\mathbf{B}_1 \mathbf{i}_2 - \mathbf{i}_{22}),$$

where the voltage current will be sought traditionally, based on Kirchhoff's second law, cf. Fig. 2.

$$(8) \frac{d\mathbf{i}_{22}}{dt} = \mathbf{L}_2^{-1}(\mathbf{u}_2 - \mathbf{R}_2 \mathbf{i}_{22}).$$

Now let's consider a mathematical model of a distributed parameter transmission line. For the sake of a more effective implementation of the line's digital model when analysing transient processes, using the column vector of the voltage function as the generalised coordinate is recommended. A second-order partial differential equation of voltage will be employed for this purpose to build the mathematical line model.

The boundary conditions of the third type, Kirchhoff's second law for distributed parameter circuits, will be expressed in line with [11]:

$$(9) -\frac{\partial \mathbf{u}(x,t)}{\partial x} = \mathbf{R}_0 \mathbf{i}(x,t) + \mathbf{L}_0 \frac{\partial \mathbf{i}(x,t)}{\partial t}.$$

For the  $N^{\text{th}}$  node, the discrete form of (9) will be formulated according to the central discretisation of the spatial derivative [11]:

$$(10) -\frac{\mathbf{u}_{N+1} - \mathbf{u}_{N-1}}{2\Delta x} = \mathbf{R}_0 \mathbf{i}_N + \mathbf{L}_0 \frac{d\mathbf{i}_N}{dt},$$

where:  $\mathbf{u}_{N+1}$  – virtual voltage across a fictitious discretization node.

$$(11) \frac{\partial^2 \mathbf{u}}{\partial t^2} = (\mathbf{L}_0 \mathbf{C}_0)^{-1} \left( \frac{\partial^2 \mathbf{u}}{\partial x^2} - (\mathbf{L}_0 \mathbf{g}_0 + \mathbf{R}_0 \mathbf{C}_0) \frac{\partial \mathbf{u}}{\partial t} - \mathbf{R}_0 \mathbf{g}_0 \mathbf{u} \right),$$

where:  $\mathbf{R}_0, \mathbf{L}_0, \mathbf{g}_0, \mathbf{C}_0$  – the matrixes of line parameters.

$$(12) \mathbf{L}_0 \equiv \begin{bmatrix} L_0 & M & M \\ M & L_0 & M \\ M & M & L_0 \end{bmatrix}, \quad \mathbf{R}_0 \equiv \begin{bmatrix} R_0 + R_{0Z} & R_{0Z} & R_{0Z} \\ R_{0Z} & R_0 + R_{0Z} & R_{0Z} \\ R_{0Z} & R_{0Z} & R_0 + R_{0Z} \end{bmatrix}$$

$$\mathbf{C}_0 = \begin{bmatrix} C_0 + 2C & -C & -C \\ -C & C_0 + 2C & -C \\ -C & -C & C_0 + 2C \end{bmatrix}, \quad \mathbf{g}_0 = \begin{bmatrix} g_0 + 2g & -g & -g \\ -g & g_0 + 2g & -g \\ -g & -g & g_0 + 2g \end{bmatrix}$$

Discretising (12) results in:

$$(13) \quad \frac{dv_j}{dt} = (\mathbf{L}_0 \mathbf{C}_0)^{-1} \left[ \frac{1}{(\Delta x)^2} (\mathbf{u}_{j+1} - 2\mathbf{u}_j + \mathbf{u}_{j-1}) - (\mathbf{L}_0 \mathbf{g}_0 + \mathbf{r}_0 \mathbf{C}_0) \mathbf{v}_j - \mathbf{r}_0 \mathbf{g}_0 \mathbf{u}_j \right], \quad \frac{d\mathbf{u}_j}{dt} = \mathbf{v}_j, \quad j=1, \dots, N.$$

$\mathbf{u}_{N+1}$  is calculated as per (10).

Calculating the current across the line elements is an important functional dependence. (9) is discretised differently: the first right-hand side spatial derivative [11]:

$$(14) \quad \frac{d\mathbf{i}_j}{dt} = -\mathbf{L}_0^{-1} \left( \frac{\mathbf{u}_{j+1} - \mathbf{u}_j}{\Delta x} + \mathbf{R}_0 \mathbf{i}_j \right), \quad j=1, \dots, N-1.$$

Note (14) is not used in the iteration process as an element of a differential equation system. The integration of this equation, on the other hand, is for a purely informative purpose of illustrating the current function across the supply line for a particular value of  $j$ .

The following system of differential equations: (5) – (8), (13) is integrated jointly considering (1), (2), (10), and (12).

### Computer simulation results

This is the sequence of the computer simulation: at  $t = 0$ s, the power line is switched on at its rated power considering the nature of controlled switching, in particular. It's turned on at time intervals for momentary phase voltages to be zero. After reaching the steady state, the supply phase C to the power transformer T4 at K in Figure 1 is switched off at  $t = 0.06$  s.

These are the parameters of the electric power system.

The power supply line:  $l = 476$  km,  $r_0 = 1.9 \cdot 10^{-5}$   $\Omega$ /m,  $L_0 = 1.665 \cdot 10^{-6}$  H/m,  $C_0 = 1.0131 \cdot 10^{-11}$  F/m,  $g_0 = 3.25 \cdot 10^{-11}$  Sm/m,  $C = 1.0122 \cdot 10^{-12}$  F/m,  $g = 3.25 \cdot 10^{-13}$  Sm/m,  $r_z = 5 \cdot 10^{-5}$   $\Omega$ /m,  $M = 7.41 \cdot 10^{-7}$  H/m.

Autotransformers: T1 – T3 750/330 kV:  $r_1 = 0.49$   $\Omega$ ,  $r_2 = 1.36$   $\Omega$ ,  $L_1 = 0.188$  H,  $L_2 = 0.313$   $\Omega$ ,  $L_m = 0.177$  H.

Transformer T4: U = 330/24 kV:  $r_1 = 0.13$   $\Omega$ ,  $r_2 = 0.00068$   $\Omega$ ,  $L\sigma_1 = 0.21$  H,  $L\sigma_2 = 0.0001$  H,  $L_m = 0.088$  H.

Equivalent load:  $R_A = R_B = R_C = 12.5$   $\Omega$ ,  $L_A = L_B = L_C = 0.027$  H,  $C_A = C_B = C_C = 0.000002$  F.

Supply voltages:  $e^{(A)} = 632 \sin(\omega t)$  kV,  $e^{(B)} = 632 \sin(\omega t - 120^\circ)$  kV,  $e^{(C)} = 632 \sin(\omega t + 120^\circ)$  kV.

The current and voltage waveforms in Figures 3–7 are coloured as follows: phase A – yellow, phase B – green, phase C – red.

Figure 3 depicts currents in the last discrete branch of the line. A virtual absence of inrush currents can be noted, owing to the controlled switching of the power line. Once the system reaches its steady state, the phase current amplitudes are 1.26 kA. After phase C near the transformer T4 is off, that phase's current becomes zero across the line, the amplitude of phase B current remains virtually the same, and of the phase A current reduces to 1.13 kA.

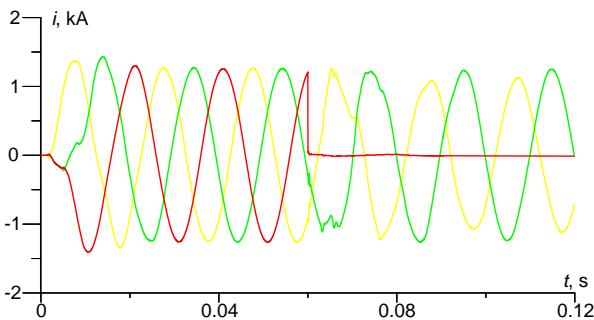


Fig. 3. Currents across the last discretisation branch

The time waveforms of phase voltages mid-power transmission line are shown in Figure 4.

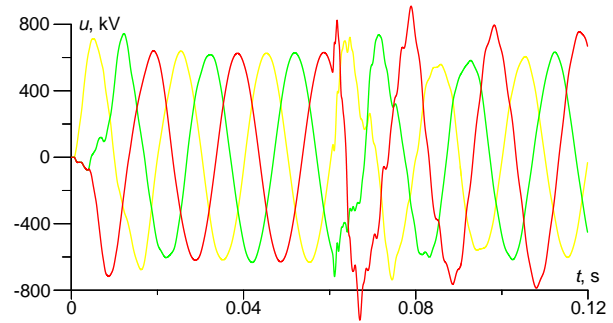


Fig. 4. Voltage mid-line

The voltage amplitudes are 631 kV on reaching the steady state. After phase C is off and at the end of the transient process, phase A voltage amplitude diminishes to 610 kV. The voltage remains unchanged in phase B. As far as phase C is concerned, a clear Ferranti effect can be observed, since phase C is in fact idle. Its amplitude rises to 757 kV, or by 17% more than the maximum acceptable working phase voltage, i.e., 642 kV.

Figure 5 presents currents across the primary windings of transformer T4. In normal steady state, the amplitudes of T4's currents are 3.31 kA. Once phase C is off, phase A and B currents phase-shift and become counterphase, with an amplitude of 2.84 kA.

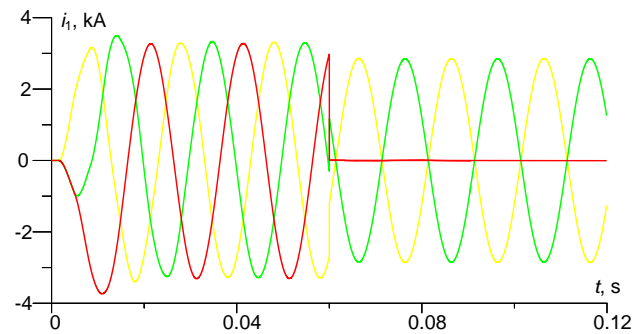


Fig. 5. Currents across the primary windings of T4

The voltage waveforms of T4's secondary windings, shown in Figure 6, are quite interesting.

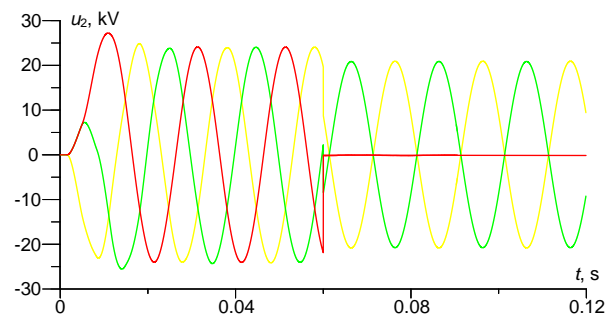


Fig. 6. The voltage of T4's secondary winding

It can be seen the voltages across T4's secondary winding have an amplitude of 23.6 kV in the normal steady state. After phase C of the primary winding is switched off, the phase C voltage is zero, and the voltages of phases A and B are in counter-phase at an amplitude of 21 kV.

The voltage waveforms across the transformer's equivalent load are illustrated in Figure 7.

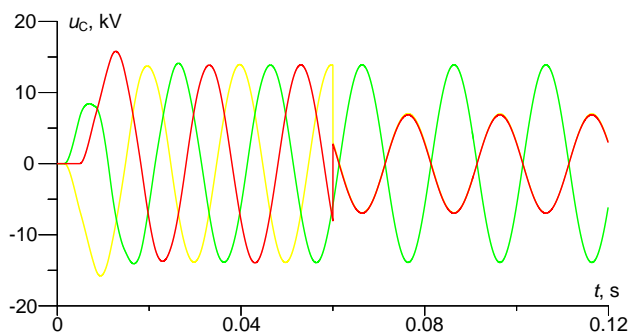


Fig. 7. Voltages across the transformer's equivalent load

Voltages across the transformer's equivalent load have an amplitude of 13.6 kV in the steady state; after the phase is off, the phase B voltage remains the same, while phase A and C voltages are in phase. Phase A and C voltage waveforms are identical and the amplitudes are 6.6 kV in Figure 7.

### Conclusion

The mathematical model of an electric line section developed in this paper, with a transformer as its key part, helps analyse transient processes in the asymmetrical operation states of the system, in particular, when the transformer is in open-phase operation. The model allows for a computer simulation of transient processes and an assessment of the impact of multiple factors on the network's stable operation, as affirmed by computer simulation results.

The application of a software code based on the mathematical model allows for a detailed analysis of the grid's operation in normal and emergency conditions. This paves the way for a continuous improvement to the methods of grid management and monitoring, which is of a potentially high importance to enhancing their reliability and performance.

**Authors:** dr hab. inż. Andriy Chaban, prof. URad., Faculty of Transport, Electrical Engineering and Computer Science, Casimir Pulaski Radom University, ul. Malczewskiego 29, 26-600 Radom, Institute of Power Engineering and Control Systems, Lviv Polytechnic National University, ul Bandery 12, Lwów, Ukraine, Department of Electrical Systems, Lviv National Environmental University, ul. W. Wielkiego 1, Dubliany, E-mail: atchaban@gmail.com; dr inż. Andrzej Szafraniec, prof. URad., Faculty of Transport, Electrical Engineering and Computer Science, Casimir Pulaski Radom University, ul. Malczewskiego 29, 26-600 Radom, ul. Malczewskiego 29, 26-600 Radom, E-mail: a.szafraniec@uthrad.pl; dr inż. Vitaliy Levoniuk, Department of Electrical Systems, Lviv National Environmental University, ul. W. Wielkiego 1, Dubliany, Ukraine, E-mail: bacha1991@ukr.net;

Prof. dr hab. inż. Andrzej Lewiński., Faculty of Transport, Electrical Engineering and Computer Science, Casimir Pulaski Radom University, ul. Malczewskiego 29, 26-600 Radom, E-mail: a.lewinski@uthrad.pl, dr inż. Marek Chmiel, Faculty of Electrical Engineering, Czestochowa University of Technology, 42-201 Czestochowa, al. Armii Krajowej 17, E-mail: marek.chmiel@pcz.pl.

### LITERATURA

- [1] Chaban, A.; Lis, M.; Szafraniec, A.; Levoniuk, V., Mathematical Modelling of Transient Processes in a Three Phase Electric Power System for a Single Phase Short-Circuit. *Energies*, (2022), 15, 1126
- [2] Chaban A., Lis M., Szafraniec A., Chrzan M., Levoniuk V., Interdisciplinary modelling of transient processes in local electric power systems including long supply lines of distributed parameters, *IEEE Xplore*, (2018) Applications of Electromagnetics in Modern Techniques and Medicine (PTZE), 17-20
- [3] Surdacki P., Jaroszyński L., Woźniak Ł., Modelowanie prądu włączania transformatora nadprzewodnikowego w środowisku Pspice, *Przegląd elektrotechniczny*, (2021), nr 4, 162 – 165
- [4] Furgał J., Kuniewski, M., Pająk P., Analysis of internal overvoltages in transformer windings during transients in electrical networks, *Energies*, (2020), 13, 2644
- [5] Levačić G., Ivanković I., Čurin M., Mathematical model of power transmission network for calculations in frequency domain, Proceedings of the 2nd International Colloquium on Smart Grid Metrology (SMAGRIMET) (2019), 09-12 April 2019, Split, Croatia.
- [6] Bulucea C.A., Nicola D.A., Mastorakis N.E., Cismaru D.C., Modelling of electrical transformers in dynamic regimes. Proceedings of the 9th WSEAS/IASME International Conference on electric power systems, high voltages, electric machines, (2009), Genova, Italy. October 17-19, 2009, 188-195.
- [7] Vakhnina V. V., Kuznetsov V. N., Shapovalov V. A., Modeling the saturation processes of a power-transformer core under simultaneous direct and alternating current passing through the winding, *Electrical Engineering*, (2017), 88, 223–228
- [8] Varricchio S. L., Gomes Jr S., Rangel R. D., Three winding transformer s-domain model for modal analysis of electrical networks, *International Journal of Electrical Power & Energy Systems*, (2011), Volume 33, Issue 3, 420-429
- [9] Bosneaga V. A., Suslov V. M., Investigation of asymmetrical modes of three-phase three leg transformer with windings connection in zigzag, *Regional energy problems*, (2013). Nr 2, 22, 38-45 (Rus).
- [10] Shcherbak, I. Mathematical model of consumer regulators management for alignment of electric load graphs of transformer substation 10/0.4 kV, *Lighting Engineering & Power Engineering*, (2020), 3(56), 125–129
- [11] Chaban A., Hamilton-Ostrogradski Principle in Electromechanical Systems; *Soroki*, Lviv, Ukraine, ((2015), 488.